

# Enhanced Image Differencing for Precise Change Detection in Static Environments

Yohei Nishidate \* , Yukihide Kohira, Shigeo Takahashi, Rentaro Yoshioka

## Abstract

This study addresses the challenge of detecting subtle changes in static environments, specifically focusing on images taken at different times in a museum. Typically, the method based on direct image differencing and thresholding for change detection encounters limitations due to high rates of false positives and difficulty in discerning subtle changes. To improve accuracy, we employed enhanced correlation coefficient (ECC) maximization with a perspective transformations model for image alignment. Also, we developed a color adjustment methodology combining *Lab* color scale conversion with CLAHE equalization in harmonizing color intensity under varied lighting conditions. Experiments conducted at the Fukushima Prefectural Museum with images from 11 locations demonstrated the effectiveness of our methods in detecting a range of changes, from object displacements to lighting variations. The study highlights the potential of these techniques in applications requiring precise change detection in static settings, with recommendations for future work aimed at refining these approaches for broader scenarios and challenging lighting conditions.

**Keywords:** Change detection, Low computational cost, Multi-temporal images, Remote surveillance.

## 1 Introduction

Change detection plays a crucial role in discerning and quantifying environmental modifications, land use changes, urban development, and the management of natural resources. In the realm of remote sensing, change detection is instrumental in understanding the dynamics of land cover, deforestation, agricultural expansion, and urbanization [1, 2, 3, 4]. This technique is also vital in environmental monitoring, disaster management, and evaluating the impacts of climate change [5]. Similarly, in video surveillance, tracking changes across consecutive frames aids in the detection of human activities [6]. In the medical field, change detection enables the comparison of images taken at different times, thereby facilitating the tracking of disease progression or recovery [7, 8, 9].

Historically, change detection has predominantly relied on pixel-based methods, which primarily involve the direct subtraction or ratioing of pixel values from multi-temporal images. While these rudimentary techniques have exhibited moderate success, they are prone

---

\* The University of Aizu, Aizu-Wakamatsu, Japan

to producing a high rate of false positives, especially in dynamically changing environments [10]. Machine learning has revolutionized numerous fields, including change detection. The enhancement in the quality and accessibility of satellite, aerial, and ground-based imagery has led to the development of more sophisticated change detection methods that incorporate advanced machine learning algorithms [11, 12]. Despite their advantages in accuracy and efficiency, these techniques often come with challenges, such as extensive data preparation, high computational costs, and significant energy consumption.

There are two primary advantages of artificial intelligence techniques over direct image differencing for detecting changes in images. The first is the susceptibility of direct differentiation to failures due to minor variations in camera configurations or image distortions. The second concerns the impact of changes in image tone, influenced by lighting conditions, white balance, and camera sensor sensitivity, leading to detection inaccuracies. While machine learning techniques are beneficial when sufficient computational resources are available, their applicability becomes limited in resource-constrained environments, such as edge devices. In other words, there is a possibility of the method based on direct image differencing being advantageous if it can handle these two difficulties.

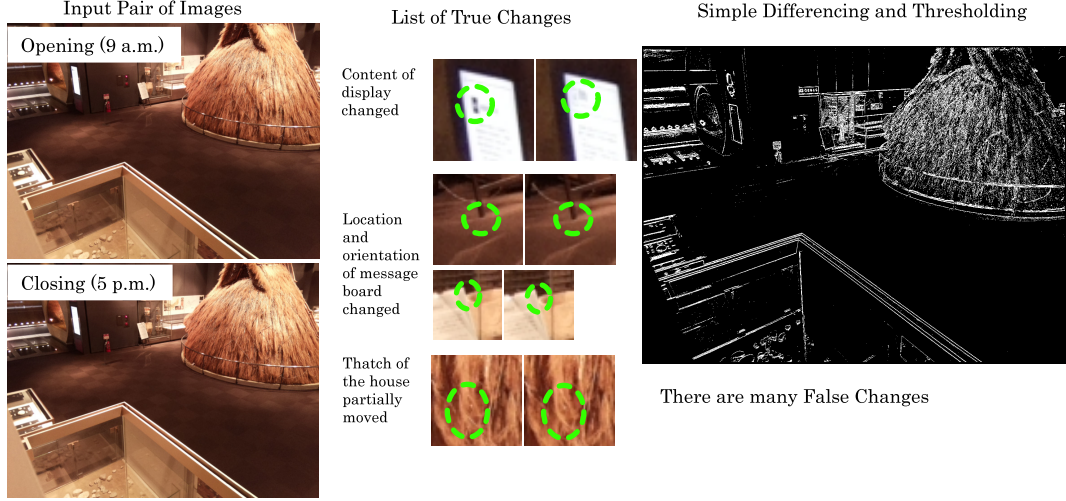
In this context, our study focuses on the development of a computationally efficient algorithm for change detection in image pairs based on direct image differencing and thresholding. We aim to create an algorithm that is not only less demanding computationally but also capable of running on single-board computers equipped with sensors, such as Raspberry Pi devices, in exhibition environments. This approach addresses the need for a balance between computational efficiency and the flexibility of change detection methods in resource-limited settings.

## 2 Drawbacks of direct differencing and thresholding

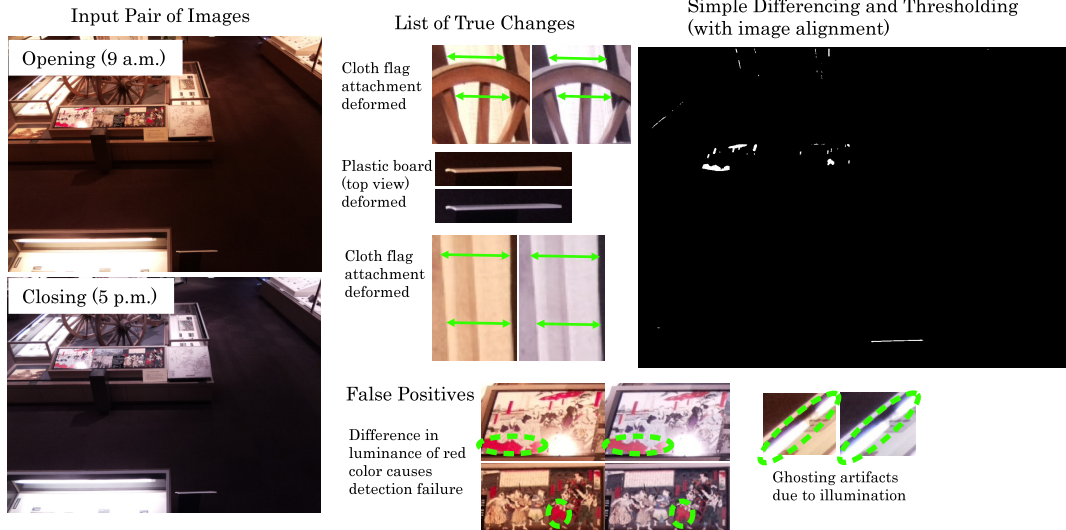
In this study, we address the task of visualizing changes that occur within a relatively static environment over a certain period. Our methodology is centered on the comparison of paired images, such as those taken at the begin and end of operating hours in the exhibition rooms of a museum. By contrasting these images, we are able to identify and highlight pixel-level changes. This approach promises to enable curators or security officers to efficiently detect and address any alterations to objects, ensuring the integrity and safety of the exhibits. This technique has the potential to serve as a proactive measure in museum management, allowing for the swift identification and correction of any discrepancies or potential issues with the displayed items. The fundamental approach we consider is a straightforward one: transforming the images to grayscale, computing the pixel differences, and identifying pixels where this difference surpasses a predefined threshold. Figure 1(a) illustrates an example of this technique.

However, a significant challenge arises when attempting to visually discern changes directly from the input images. Our preliminary results reveal that while the basic approach of differencing and thresholding detects many changes, the majority of these are false positives. These inaccuracies predominantly stem from minor physical displacements of the camera, likely caused by vibrations, resulting in slight shifts and distortions between the images. We will delve deeper into image alignment algorithms suitable for our needs in Section 3.

Assuming that the effective alignment of the images is achievable, we encounter another issue related to variations in color tones. Figure 1(b) presents an example in which



(a) An example without image alignment



(b) An example with image alignment but no color adjustment

Figure 1: Illustration of change detection via image differencing and thresholding. Panel (a) demonstrates the method without image alignment, and Panel (b) corresponds to the method with image alignment but under different color temperatures. For each case, the left pair of images represents the input pair of images captured at the opening and closing times of the museum. The list of true changes is shown in the center as an enlarged view of the changed regions. The rightmost image in each panel shows the outcome of the change detection process.

this simple differencing and thresholding method is applied to well-aligned images. In this instance, the deformation of large fabric flags on the wall due to air conditioning is successfully detected. However, a prominent issue arises with luminance differences, particularly in the crimson color region, leading to varying intensities in the grayscale images and, consequently, significant detection errors. An approach to address this challenge will be discussed in Section 4.

### 3 Image alignment

Image registration, a process critical for aligning multiple images of the same scene captured under different conditions or at various times, plays a central role in this study. We explored two image registration algorithms. The first method, based on the approach in [13], employs phase correlation and logarithmic scaling to ascertain rotation, scaling, and translation parameters for alignment. This process begins with converting images to grayscale, followed by applying a high-pass filter for preprocessing. Subsequently, the fast Fourier transform (FFT) and log-polar transformation are utilized to determine the necessary rotation and scaling. The translational shift is then computed using the phase correlation technique. This method essentially seeks to find the affine transformation.

The second algorithm that we investigated is the enhanced correlation coefficient (ECC) maximization [14]. The ECC, which is robust against illumination changes and capable of handling linear and non-linear intensity variations, is particularly effective in environments with fluctuating lighting conditions [15]. Despite its iterative nature, the ECC algorithm demonstrates strong convergence properties, often yielding precise registration outcomes. It also offers flexibility in the choice of transformation models, with this study employing a perspective transformation (homography) model. While the transformation matrix resembles those in the affine model, the homography model takes perspective distortion corrections into account.

Figure 2 presents a comparative analysis of two image registration algorithms across two distinct examples. The first row features the same scene as depicted in Fig. 1(a), where the expected differences have been previously established. The second row shows a benchmarking scenario, a scene where ideally no differences should be detected if the images are accurately aligned. The leftmost image in this row serves as a reference, showing the outcome when no image alignment is applied. In the unaligned scenario, a multitude of detection failures are evident, particularly around object edges within the scene. The FFT-based phase correlation technique, on the other hand, successfully identifies actual changes in specific elements, such as the electric bulletin board, the message board, and the thatch of the house. However, this method still presents several detection errors in areas where no actual changes have occurred. Conversely, the ECC maximization method excels by accurately detecting all changes without any false positives.

To summarize, while the FFT-based phase correlation technique demonstrates computational efficiency in handling affine transformations, the ECC maximization method proves more robust against image distortions since it offers greater flexibility in selecting different transformation models. This flexibility is particularly beneficial for accommodating image distortions caused by perspective projection effects, going beyond the capabilities of mere affine transformation handling.

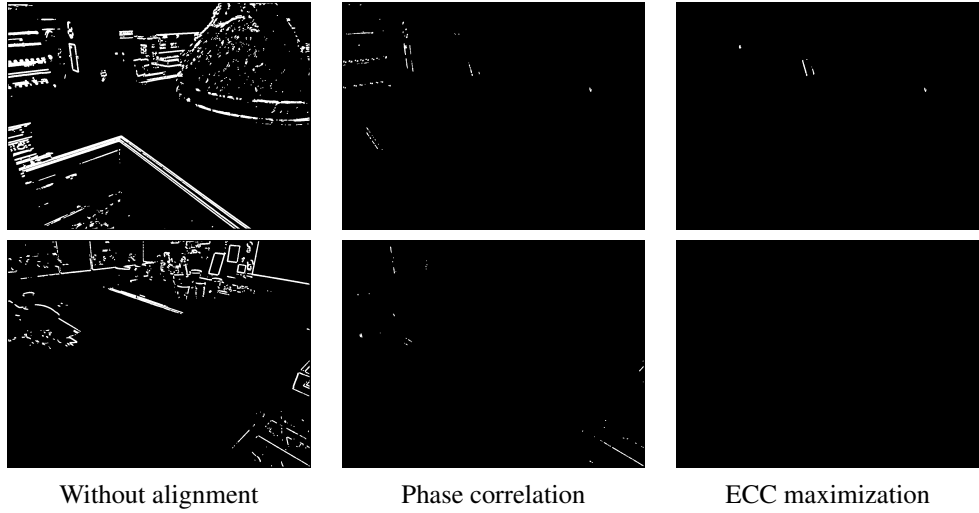


Figure 2: Difference detection in two example scenes. Differences identified in the images are highlighted in white. The left column displays results obtained without image alignment, demonstrating numerous detection errors, especially around object edges. The results in the center column, obtained by employing the phase correlation technique [13], show improved detection accuracy, identifying actual changes but still presenting some errors. The images in the right column, obtained using the ECC maximization method [14], exhibit superior performance with accurate detection of changes and no false positives.

## 4 Color adjustment

Adjusting the color tones of images is a fundamental step to achieving precise image alignment and effective difference detection. This necessity is evident in the example shown in Fig. 1(b), where the color temperature, influenced by the lighting conditions, leads to detection errors. By harmonizing the color tones, the image registration process can be simplified, as this reduces the complications arising from color variations.

In the context of our study, harmonizing the intensity of images when converting them to grayscale proves to be sufficient. To achieve this, white balancing and color constancy algorithms emerge as the primary methods for color adjustment. These techniques are particularly appealing for our application as they not only fulfill the requirement of harmonizing color tones but also offer the advantage of being computationally efficient.

### 4.1 ITU conversion

To establish a baseline for our study, we utilized a standard grayscale conversion technique recommended by the International Telecommunication Union (ITU) [16]. This method is defined by the equation:

$$Y(x,y) = 0.299R(x,y) + 0.588G(x,y) + 0.114B(x,y), \quad (1)$$

where  $Y(x,y)$  is the color intensity of the converted grayscale image at pixel  $(x,y)$ ,  $R(x,y)$ ,  $G(x,y)$ , and  $B(x,y)$  are the color intensities of the red, green, and blue components, respectively, at the same pixel. This approach provides a straightforward and widely accepted method for converting color images to grayscale.

## 4.2 Gray World algorithm

The Gray World algorithm is a simple and widely-used color constancy algorithm for automatic white balance adjustment in digital images [17]. This algorithm operates on the fundamental assumption that the average color of a scene, when averaged across all pixels, approximates a gray tone. More specifically, it posits that the mean intensity for each of the primary color channels—red, green, and blue—is equal. To apply this algorithm, each color channel is scaled according to its average intensity across the entire image. This process helps in correcting the color balance, thereby bringing the overall color tone of the image closer to a neutral gray.

## 4.3 Multi-Scale Retinex

The Retinex algorithm, rooted in the principles of human visual perception, serves as an effective color constancy method to enhance the visibility and appearance of digital images [18]. This algorithm improves the dynamic range and corrects the color balance of images by focusing on the concept that the perceived color of an object is influenced more by the light it reflects than the color of the light source itself. By distinguishing between the illuminant and reflectance components of an image, Retinex effectively enhances the dynamic range and corrects the color balance, resulting in more visually appealing images [19, 20]. The single-scale Retinex (SSR) version of this algorithm is calculated using the following equation:

$$R_i(x, y) = \log [I_i(x, y)] - \log [I_i(x, y) * F(x, y)], \quad (2)$$

where  $R_i(x, y)$  is the Retinex value for  $i$ -th color channel,  $I_i(x, y)$  is the  $i$ -th color channel of the input image, and  $F(x, y)$  is the normalized surround function, often chosen to be a radial function. In our research, we have opted for a Gaussian filter as the surround function.

Furthermore, the Multi-Scale Retinex (MSR) is an extension of SSR, which involves calculating a weighted average of SSR values across different standard deviations. For instance, in our study, we adopted three standard deviation values of the Gaussian filter  $\sigma = (15, 80, 250)$  with equal weighting  $w_n = 1/3$ , as employed in previous works [19, 20]. Details of the algorithm can be found in [21].

## 4.4 Multi-Scale Retinex with Chromaticity Preservation

A notable limitation of the MSR algorithm is its tendency to produce images with desaturated colors. To counter this issue, the Multi-Scale Retinex with Color Restoration (MSRCR) has been developed, offering enhancements in image brightness and contrast while simultaneously preserving or restoring the original colors of the image [19, 20]. This approach effectively reinstates the vibrant colors that might be lost in the MSR process, thereby rendering images more natural and closer to the human eye's perception in similar lighting conditions.

However, a challenge identified with the MSRCR, as highlighted in [21], is its handling of images with saturated colors. In such cases, pixels with intensity values near the extremes (near 0 or 255) may undergo drastic shifts to the opposite end of the spectrum. To address this and fulfill the objectives of the Retinex theory more effectively, the Multi-Scale Retinex with Chromaticity Preservation (MSRCP) was developed. The MSRCP is designed to enhance images in accordance with the Retinex theory while maintaining the

chromaticity of the image, thus preventing the issue of color desaturation and ensuring a more balanced and true-to-life color representation in the processed images.

#### 4.5 Lab conversion with CLAHE equalization

In our research, we developed and tested a simple method aimed at adjusting illumination intensity in digital images. This method begins by converting the RGB color image into the *Lab* color scale. The *Lab* color space is particularly advantageous for this task due to its ability to separate the lightness (L) component from the color components.

Once the image is converted to the *Lab* scale, we specifically target the L (lightness) component for adjustment. This adjustment is carried out using contrast-limited adaptive histogram equalization (CLAHE), a technique noted for its efficacy in enhancing image contrast [22, 23]. CLAHE is renowned for its application in diverse fields, such as medical image processing, remote sensing, and computer vision. The primary advantage of CLAHE lies in its ability to adapt the intensity mapping of an image according to local variations. This localized approach allows CLAHE to enhance contrast effectively while avoiding the over-amplification of noise in low-contrast areas and preserving the inherent contrast in high-contrast regions.

#### 4.6 Comparisons

Figure 3 provides a comparative analysis of the aforementioned color synchronization methods utilized to equalize the intensity of images captured under different color temperature conditions. In this context, it is crucial to underline that our primary objective is to ensure that the color intensities of identical objects in different images are either equalized or brought as close to equality as possible.

In Fig. 3 (a) to (c), three pairs of images are displayed. The first pair (a) shows the original input color images. The second pair (b) is the result of applying the grayscale conversion recommended by the ITU [16], serving as a baseline for comparison. The third pair (c) is processed using the Gray World algorithm. These methods aim to demonstrate how basic grayscale conversion techniques perform in terms of color tone harmonization. Fig. 3 (d) to (f) presents three additional pairs of images processed with advanced techniques. The first pair (d) is processed using the MSR method [19, 20], known for its effectiveness in various lighting conditions. The second pair (e) is the result of using the MSRPCP [21], which addresses some of the color saturation issues observed in the MSR. Lastly, the third pair (f) in this row is obtained through RGB to *Lab* conversion followed by CLAHE equalization applied to the L-component, illustrating the effectiveness of our proposed method in achieving color tone harmonization.

In the evaluation of the different color-conversion methods used in our study, it was observed that the color of objects appeared similar across most pixels in all methods. However, noticeable disparities in the intensity of the gray color were found in specific regions, particularly those where the original color was a vivid crimson. These differences were especially pronounced in the simple grayscale conversion recommended by the ITU and the method based on the Gray World assumption. While MSR methods are generally considered robust to brightness variations and effective under diverse lighting conditions, they also exhibited noticeable differences in color intensity in our specific case. In contrast, our method demonstrated superior performance in harmonizing color intensity for grayscale images. This method effectively addressed the challenges posed by variations in lighting

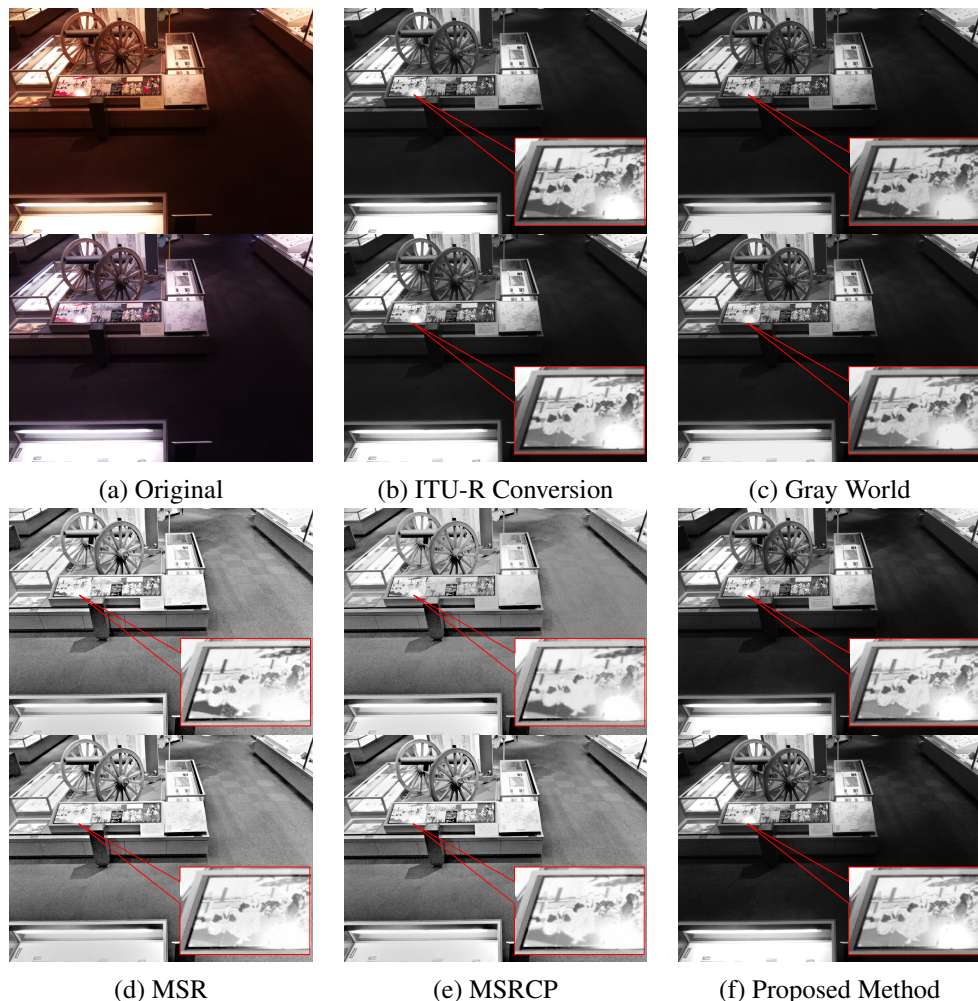


Figure 3: Comparative results of various color adjustment methods. Each figure consists of two rows, showing pictures at the opening (9:00) and closing times (17:00) of a venue.

and color temperature, leading to more consistent and harmonized grayscale images. For the purposes of this study, we have chosen to use our *Lab* conversion and the CLAHE equalization method for color harmonization.

This comparison highlights the effectiveness of each method in achieving a consistent color intensity across images, an essential factor for accurate image registration and change detection in environments with varying lighting conditions. However, it is important to acknowledge that further investigation is required to fully assess the efficacy of this method under a variety of conditions and with different examples. This additional research will help in validating the method's versatility and effectiveness in diverse image processing applications.

## 5 Experiments

Our change detection procedure can be summarized as the following list of steps for given Images A and B:

1. Color Adjustment: Apply our color adjustment method, which includes *Lab* conversion and CLAHE equalization, to input Images A and B. The L-component of the color is used as the grayscale image intensity.
2. Perspective Projection: Calculate the perspective projection matrix using ECC maximization.
3. Image Alignment: The calculated transformation is applied to Image B to align it with Image A.
4. Gaussian Blurring: Both Images A and B are subjected to Gaussian blurring.
5. Pixel Difference Calculation: The differences between all pixels of Images A and B are calculated.
6. Thresholding: The pixels with an absolute difference in intensity exceeding a certain threshold are marked.
7. Morphological Operations: Erosion and dilation are applied to the difference image to emphasize changes.

In addition to the experiments conducted in our previous study [24], images were captured at opening and closing times at 11 different locations within the Fukushima Prefectural Museum. The locations and coverage of the 11 cameras are illustrated in Fig. 4. All images were captured at a resolution of  $1280 \times 960$  (1.2M) pixels. The computational procedure was tested on an ordinary personal computer, and in all cases, the computation was completed in approximately 600 milliseconds.

Figure 5 showcases the results of our change detection procedure, except for the results from Camera 1, which were shown above in Fig. 2.

The following list summarizes the results of our experiments:

- (a) **Camera 2:** Changes were detected in the paper box where comment sheets in the box vanished, while slight variations in illumination intensity were not detected due to thresholding.
- (b) **Camera 3:** A slightly peeled label was detected and changes observed through reflections in showcases.

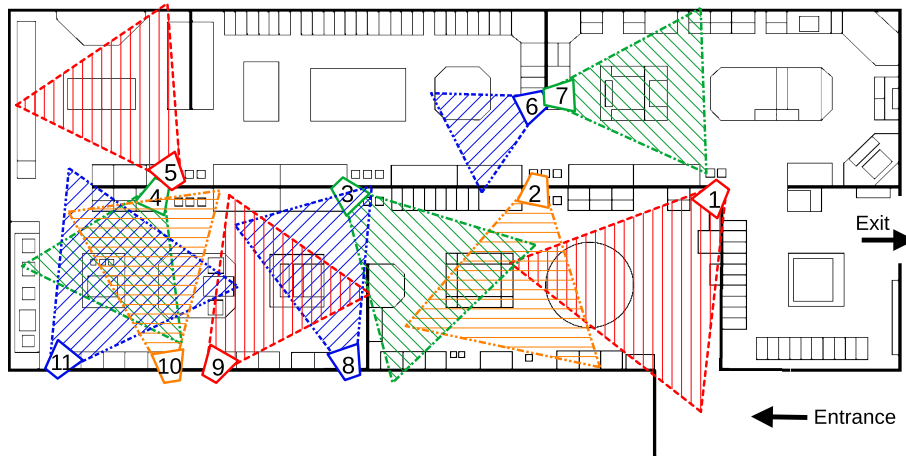


Figure 4: Locations and approximate coverage area of 11 cameras for capturing images.

- (c) **Camera 4 and (i) Camera 10:** A small object was detected with a slight directional change.
- (d) **Camera 5 and (j) Camera 11:** Changes were detected in the location of pedals for interactive exhibitions and in the armrest of a security officer's chair.
- (e) **Camera 6:** A big difference was detected in the information board due to significant rotation and deformation of the fabric cover.
- (f) **Camera 7:** This is the case in which the input images are given in different color temperatures. Changes in fabric flags and polystyrene foam board were detected, but detection failures still exist in areas with vivid crimson colors and near exhibition case lights.
- (g) **Camera 8:** Changes were successfully detected changes in a relatively dark region, demonstrating the method's effectiveness in challenging visibility conditions.
- (h) **Camera 9:** This was a control experiment with no changes in the scene.

These results demonstrate the effectiveness of our method in various settings within the museum, aiding curators and security staff in monitoring and detecting undesirable changes in exhibitions.

## 6 Conclusions

In our study, we explored the task of visualizing changes within a relatively static environment over a period, with a focus on image pairs taken at different times, such as at the opening and closing of a museum. First, we delved into image alignment techniques. We examined two algorithms for image alignment: a phase correlation technique for affine transformations and ECC maximization for perspective transformations. The comparative analysis revealed that while the phase correlation method is computationally efficient, ECC maximization provided more robust results against intensity variations and was more flexible in handling different transformation models. Another important aspect of our study was the adjustment of color tones. We explored various color adjustment methods, including ITU conversion, the Gray World algorithm, MSR, and a simple method combining *Lab*

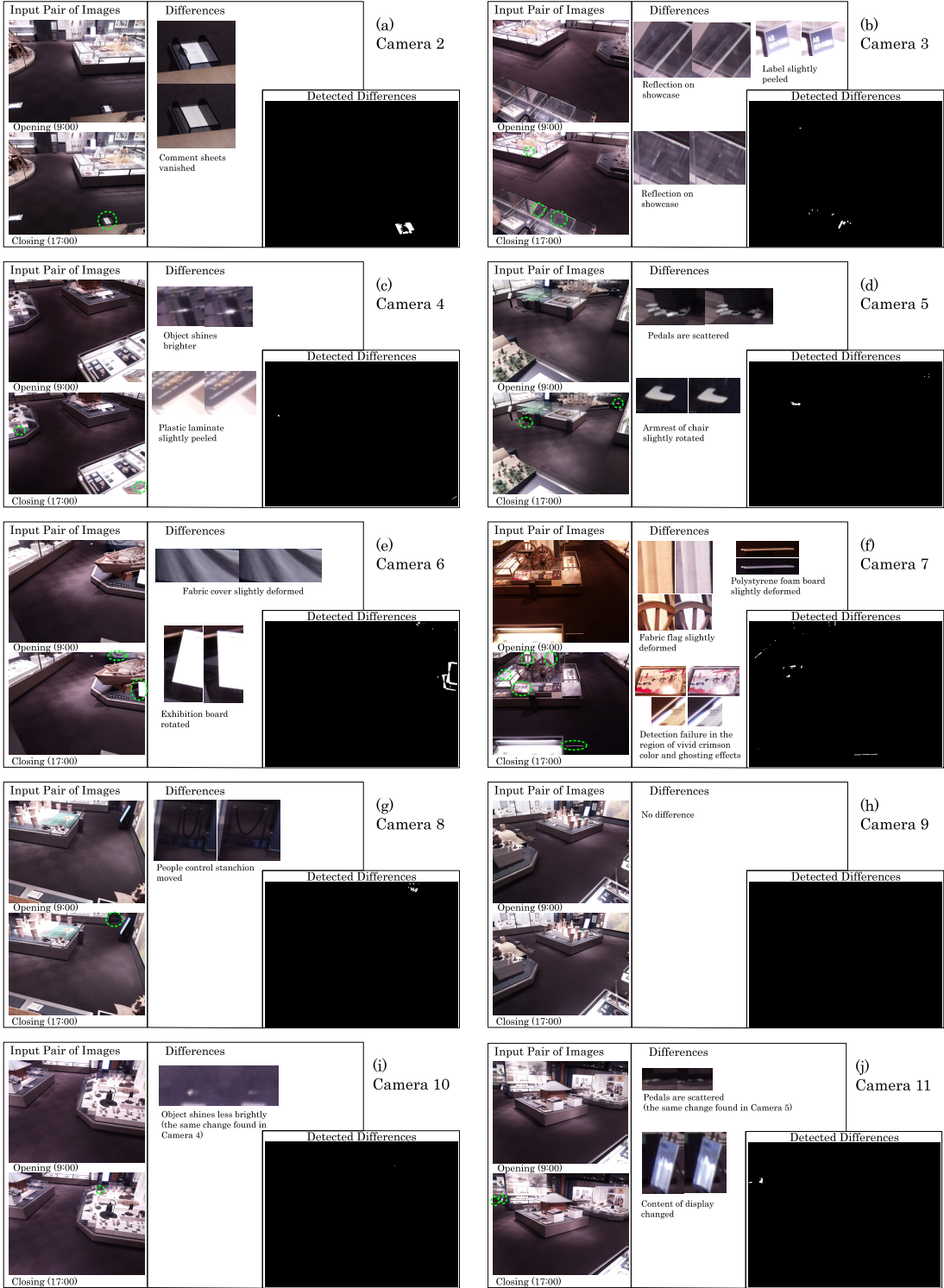


Figure 5: Results of our change detection method for images captured by Cameras 2 to 11. In all cases, we used the pictures taken at opening (9:00) and closing (17:00) times of the museum on a workday at July 7, 2022. In all cases, existing changes were successfully detected. This emphasizes the usefulness of this system in assisting curators or security officers in noticing and correcting changes if necessary.

conversion with CLAHE equalization. Our comparative analysis indicated that our *Lab* conversion and CLAHE equalization method outperformed the others in harmonizing color intensities for grayscale images.

We applied these methodologies in a series of experiments at the Fukushima Prefectural Museum, capturing images at 11 locations at opening and closing times. Our change detection procedure involved color adjustment, perspective projection, image alignment, Gaussian blurring, pixel difference calculation, thresholding, and morphological operations. The computational process was efficient: it was completed in approximately 600 milliseconds for images consisting of  $1280 \times 960$  (1.2M) pixels on an ordinary personal computer. The results demonstrated the effectiveness of our method in a range of scenarios within the museum environment. We successfully detected changes in various settings, from minor shifts in object positions to more subtle changes, such as variations in lighting and reflections. Notably, challenges persisted in areas with saturated colors and ghosting artifacts due to intense lighting, indicating areas for further research and method refinement.

In conclusion, we demonstrated the efficacy of advanced image alignment and color adjustment techniques in detecting subtle changes, which are crucial for applications such as museum security and exhibit maintenance. Future work will focus on refining these methods to address the remaining challenges and extend their applicability to a broader range of conditions and scenarios.

## Acknowledgment

We would like to express our appreciation to the Fukushima Prefectural Museum for providing access to the study environment and essential photographs, which greatly facilitated our work.

## References

- [1] Terry L. Sohl, “Change Analysis in the United Arab Emirates: An Investigation of Techniques,” Photogrammetric Engineering & Remote Sensing, vol. 65 no. 4, pp. 475-484, 1999. <https://pubs.usgs.gov/publication/70186963>
- [2] F. Yuan, K. E. Sawaya, B. C. Loeffelholz, and M. E. Bauer, “Land Cover Classification and Change Analysis of the Twin Cities (Minnesota) Metropolitan Area by Multitemporal Landsat Remote Sensing,” Remote Sensing of Environment, vol. 98, pp. 317-328, 2005. doi:10.1016/j.rse.2005.08.006
- [3] K. Sakurada and T. Okatani, “Change Detection from a Street Image Pair Using CNN Features and Superpixel Segmentation,” in Proceedings of the British Machine Vision Conference (BMVC), pp. 61.1-61.12, September 2015. doi:10.5244/C.29.61
- [4] M. A. Lebedev, Yu. V. Vizilter, O. V. Vygolov, V. A. Knyaz, and A. Yu. Rubis, “Change Detection in Remote Sensing Images Using Conditional Adversarial Networks,” International Archives of the Photogrammetry, Remote Sensing & Spatial Information Sciences, vol. 42, no. 2, pp. 565-571, 2018. doi:10.5194/isprs-archives-XLII-2-565-2018

- [5] P. Coppin, I. Jonckheere, K. Nackaerts, B. Muys, and E. Lambin, "Digital Change Detection Methods in Ecosystem Monitoring: A Review," International Journal of Remote Sensing, vol. 25, no. 9, pp. 1565-1596, 2004. doi:10.1080/0143116031000101675
- [6] C. Stauffer and W. E. L. Grimson, "Learning Patterns of Activity Using Real-Time Tracking," IEEE Transactions on Pattern Analysis and Machine Intelligence, vol. 22, no. 8, pp. 747-757, August 2000. doi:10.1109/34.868677
- [7] D. Rueckert, L. I. Sonoda, C. Hayes, D. L. G. Hill, M. O. Leach, and D. J. Hawkes, "Nonrigid Registration Using Free-Form Deformations: Application to Breast MR Images," IEEE Transactions on Medical Imaging, vol. 18, pp. 712-721, 1999. doi:10.1109/42.796284
- [8] P. A. Yushkevich, J. Piven, H. C. Hazlett, R. G. Smith, S. Ho, J. C. Gee, and G. Gerig, "User-Guided 3D Active Contour Segmentation of Anatomical Structures: Significantly Improved Efficiency and Reliability," NeuroImage, vol. 31, no. 3, pp. 1116-1128, 2006. doi:10.1016/j.neuroimage.2006.01.015
- [9] G. Litjens, T. Kooi, B. E. Bejnordi, A. A. A. Setio, F. Ciompi, M. Ghafoorian, J. A. W. M. van der Laak, B. van Ginneken, and C. I. Sánchez, "A Survey on Deep Learning in Medical Image Analysis," Medical Image Analysis, vol. 42, pp. 60-88, 2017. doi:10.1016/j.media.2017.07.005
- [10] A. Singh, "Digital Change Detection Techniques Using Remotely-Sensed Data," International Journal of Remote Sensing, vol. 10, no. 6, pp. 989-1003, 1989. doi:10.1080/01431168908903939
- [11] L. Khelifi and M. Mignotte, "Deep Learning for Change Detection in Remote Sensing Images: Comprehensive Review and Meta-Analysis," IEEE Access, vol. 8, pp. 126385-126400, 2020. doi:10.1109/ACCESS.2020.3008036
- [12] C. Benedek and T. Szirányi, "Change Detection in Optical Aerial Images by a Multilayer Conditional Mixed Markov Model," IEEE Transactions on Geoscience and Remote Sensing, vol. 47, no. 10, pp. 3416-3430, October 2009. doi:10.1109/TGRS.2009.2022633
- [13] B. S. Reddy and B. N. Chatterji, "An FFT-Based Technique for Translation, Rotation, and Scale-Invariant Image Registration," IEEE Transactions on Image Processing, vol. 5, no. 8, pp. 1266-1271, 1996. doi:10.1109/83.506761
- [14] G. D. Evangelidis and E. Z. Psarakis, "Parametric Image Alignment Using Enhanced Correlation Coefficient Maximization," IEEE Transactions on Pattern Analysis and Machine Intelligence, vol. 30, no. 10, pp. 1858-1865, Oct. 2008. doi:10.1109/TPAMI.2008.113
- [15] E. Z. Psarakis and G. D. Evangelidis, "An Enhanced Correlation-Based Method for Stereo Correspondence with Subpixel Accuracy," Tenth IEEE International Conference on Computer Vision (ICCV'05), vol. 1, Beijing, China, pp. 907-912, 2005. doi:10.1109/ICCV.2005.33

- [16] Radiocommunication Sector of International Telecommunication Union (ITU), “Studio Encoding Parameters of Digital Television for Standard 4:3 and Wide-Screen 16:9 Aspect Ratios,” Recommendation ITU-R BT.601-7, 2011. <https://www.itu.int/rec/R-REC-BT.601/>
- [17] G. Buchsbaum, “A Spatial Processor Model for Object Colour Perception,” *Journal of the Franklin Institute*, vol. 310, pp. 1–26, 1980. doi:10.1016/0016-0032(80)90058-7
- [18] E. Land and J. McCann, “Lightness and Retinex Theory,” *Journal of the Optical Society of America*, vol. 61, pp. 1–11, 1971. doi:10.1364/JOSA.61.000001
- [19] Z. Rahman, D. J. Jobson, and G. A. Woodell, “Multi-Scale Retinex for Color Image Enhancement,” in *Proceedings of 3rd IEEE International Conference on Image Processing*, Lausanne, Switzerland, 1996, pp. 1003–1006. doi:10.1109/ICIP.1996.560995
- [20] D. J. Jobson, Z. Rahman, and G. A. Woodell, “A Multiscale Retinex for Bridging the Gap Between Color Images and the Human Observation of Scenes,” *IEEE Transactions on Image Processing*, vol. 6, no. 7, pp. 965–976. doi:10.1109/83.597272
- [21] Ana Belén Petro, Catalina Sbert, and Jean-Michel Morel, “Multiscale Retinex,” *Image Processing On Line*, pp. 71–88, 2014. doi:10.5201/ipol.2014.107
- [22] J. Rosenman, C. A. Roe, R. Cromartie, K. E. Muller, and S. M. Pizer, “Portal Film Enhancement: Technique and Clinical Utility,” *International Journal of Radiation Oncology Biology Physics*, vol. 25, no. 2, pp. 333–338, 1993. doi:10.1016/0360-3016(93)90357-2
- [23] K. Zuiderveld, “Contrast Limited Adaptive Histogram Equalization,” *Graphics Gems IV*, pp. 474–485, 1994. doi:10.1016/B978-0-12-336156-1.50061-6
- [24] Y. Nishidate, Y. Kohira, S. Takahashi, and R. Yoshioka, “Precise Detection of Changes in Relatively Static Environments for Single-Board Computers,” in *Proceedings of the 14th International Congress on Advanced Applied Informatics (IIAI-AAI)*, Koriyama, Japan, 2023, pp. 57–62. doi:10.1109/IIAI-AAI59060.2023.00022 (Present paper is the extended journal version of this document).